Available online at www.sciencedirect.com
ScienceDirect
Bioorganic & Medicinal Chemistry Letters 17 (2007) 4538–4544
Bioorganic & Medicinal Chemistry Letters

Design and synthesis of hepatoselective, pyrrole-based HMG-CoA reductase inhibitors

Jeffrey A. Pfefferkorn,* Yuntao Song, Kuai-Lin Sun, Steven R. Miller, Bharat K. Trivedi, Chulho Choi, Roderick J. Sorenson, Larry D. Bratton, Paul C. Unangst, Scott D. Larsen, Toni-Jo Poel, Xue-Min Cheng, Chitase Lee, Noe Erasga, Bruce Auerbach, Valerie Askew, Lisa Dillon, Jeffrey C. Hanselman, Zhiwu Lin, Gina Lu, Andrew Robertson, Karl Olsen, Thomas Mertz, Catherine Sekerke, Alexander Pavlovsky, Melissa S. Harris, Graeme Bainbridge, Nicole Caspers, Huifen Chen and Matthias Eberstadt

Pfizer Global Research & Development, Michigan Laboratories, 2800 Plymouth Road, Ann Arbor, MI 48105, USA

Received 25 April 2007; revised 24 May 2007; accepted 30 May 2007
Available online 6 June 2007

Abstract—This manuscript describes the design and synthesis of a series of pyrrole-based inhibitors of HMG-CoA reductase for the treatment of hypercholesterolemia. Analogs were optimized using structure-based design and physical property considerations resulting in the identification of **44**, a hepatoselective HMG-CoA reductase inhibitor with excellent acute and chronic efficacy in a pre-clinical animal models.

Coronary heart disease (CHD) is the leading cause of death in the United States at an annual cost of more than $150 billion.[1] Given that hypercholesterolemia, or elevated serum cholesterol, is a key risk factor for CHD, substantial efforts have been undertaken to mitigate this condition.[2] Currently, the standard of care for treating hypercholesterolemia is the use of HMG-CoA reductase inhibitors, also known as statins, which block the rate-limiting step of cholesterol biosynthesis.[3] As a class, statins have proven remarkably safe and effective for both primary prevention of coronary heart disease and secondary prevention of coronary events.[4]

In recent years, results from several clinical trials (TNT, MIRACAL, PROVE-IT, and others) have demonstrated that increasingly aggressive LDL-C-lowering therapy may offer additional protection against CHD relative to earlier, less aggressive, treatment standards.[5] In light of this evidence, the National Cholesterol Education Program (NCEP-ATP-III) has modified its treatment guidelines recommending that highest risk CHD patients reach a treatment goal of LDL-C <70 mg/dl, down from the previous treatment goal of 100 mg/dl for this patient group.[6] Moreover, other researchers have suggested that optimal LDL-C levels to prevent atherosclerosis and CHD might be even lower, in the range of 50–70 mg/dl.[7]

Achieving such aggressive LDL-C reductions in patients typically requires the use of high dose statins alone or in combination with complimentary agents such as the cholesterol absorption inhibitor ezetimibe.[8] A potential limitation of high dose statin therapy is statin-induced myalgia, the muscle pain or weakness that sometimes accompanies statin therapy.[9] While the overall incidence of myalgia is low (2–7% of patients in trials), the likelihood of occurrence increases with drug dose, and it can be a key factor in preventing patient compliance with a treatment regimen.[9]

The mechanism of statin-induced myalgia is complex but thought to involve, in part, inhibition of HMG-CoA reductase in non-hepatic tissues (particularly

Keywords: HMG-CoA reductase inhibitor; Statin; Hypercholesterolemia.
* Corresponding author. Tel.: +1 860 686 3421; fax: +1 860 715 4608; e-mail: jeffrey.a.pfefferkorn@pfizer.com

0960-894X/$ - see front matter © 2007 Elsevier Ltd. All rights reserved.
doi:10.1016/j.bmcl.2007.05.096

muscle) resulting in the disruption of the biosynthesis of isoprenoid-derived biomolecules.[9] Encouragingly, the potential for statin-induced myalgia can be reduced by targeting HMG-CoA reductase inhibitors to hepatic tissues and limiting peripheral exposure.[10] Moreover, it has been demonstrated that the hepatoselectivity of a given HMG-CoA reductase inhibitor is related to its degree of lipophilicity.[10,11] In general, lipophilic statins tend to achieve higher levels of exposure in non-hepatic peripheral tissues, whereas more hydrophilic statins tend to be more hepatoselective. These differences in hepatoselectivity can be rationalized by the fact that lipophilic statins passively and non-selectively diffuse into both hepatocyte and non-hepatocyte cells, while hydrophilic statins rely largely on active transport into hepatocyte cells to exert their effects.[10,12] In particular the organic anion transporting polypeptide (OATP) family of membrane transporters has been reported to be important for the hepatic uptake of hydrophilic statins such as rosuvastatin and pravastatin.[10d,12]

Given this precedent, we recently undertook a discovery effort to identify novel, potent, and hepatoselective HMG-CoA reductase inhibitors which might be useful in helping patients reach increasingly aggressive LDL-C reduction goals. We sought to accomplish this through modification of the atorvastatin (**1**) template with a focus on altering the central pyrrole heterocycle. These efforts included replacement of the pyrrole with alternative 5-membered heterocycles as reported elsewhere[13] as well as the evaluation of an isomeric pyrrole core represented by prototype inhibitor **2** (Fig. 1). Comparison of atorvastatin (**1**) and **2** illustrates the transposition of the 3,5-dihydroxyhexanoic acid side chain from the 1-position (atorvastatin) to the 2-position of the central pyrrole of **2**. Herein, we describe the structure–activity studies undertaken on inhibitor **2** aimed at optimizing hepatoselectivity and efficacy.[14]

Schemes 1 and 2 illustrate the synthesis of prototype inhibitor **2** as a representative example of this series of inhibitors. As shown, a Barton–Zard synthesis was utilized for construction of the central pyrrole heterocycle.[15] Initially, 4-fluorobenzyl bromide (**4**) was treated with silver nitrite to afford 1-fluoro-4-nitromethyl-benzene (**5**). In parallel, 4-fluorobenzaldehyde (**6**) was converted to imine **8** by treatment with *n*-butylamine. Subsequent reaction of **5** and **8** in acetic acid afforded nitro-olefin **10**. To complete the pyrrole synthesis, intermediate **10** was reacted with ethyl isocyanatoacetate in the presence of DBU to generate pyrrole **11** in modest yield. N-Alkylation of **11** was then accomplished using *i*-propyl iodide and powdered KOH in DMSO to provide pyrrole **12**, which was subjected to Vilsmeier–Haack formylation to afford pyrrole carboxaldehyde **13**. Finally, the ester of **13** was saponified with aqueous NaOH to generate carboxylic acid **14** as a key intermediate for subsequent analog synthesis.

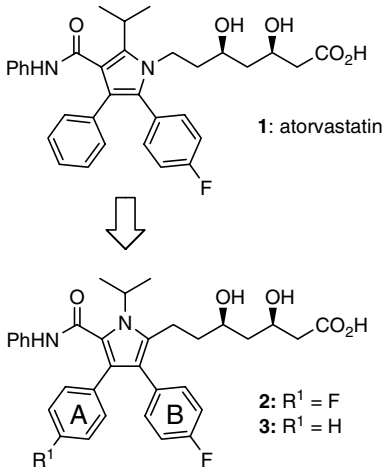

Figure 1. Structures of atorvastatin (**1**) and isomeric HMG-CoA reductase inhibitors **2** and **3**.

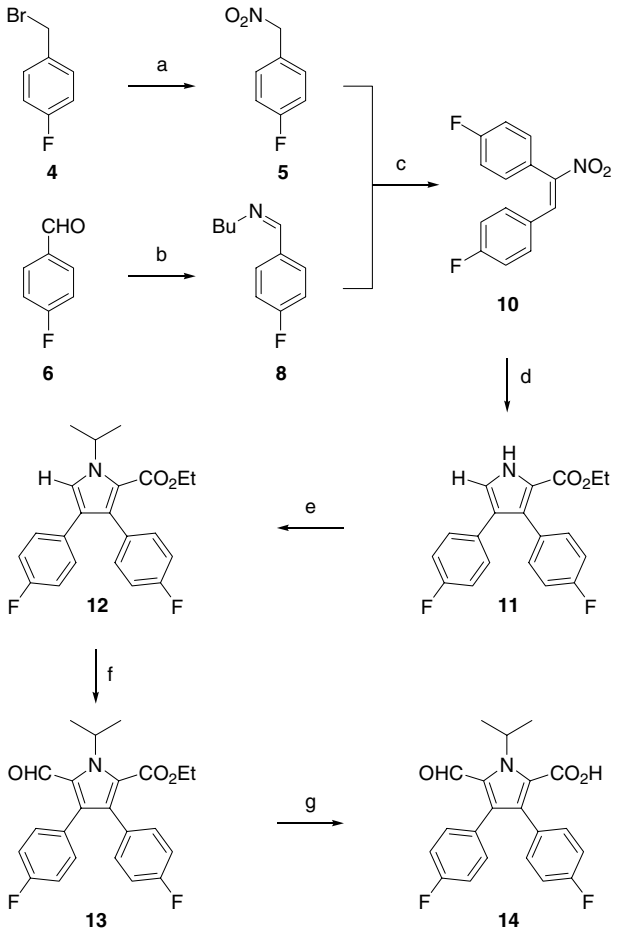

Scheme 1. Synthesis of functionalized pyrrole **14**. Reagents and conditions: (a) $AgNO_2$, Et_2O, 0 °C, 12 h, 36%; (b) *n*-$BuNH_2$, C_6H_6, 80 °C, 2 h, 100%; (c) AcOH, 25 °C, 12 h, 82%; (d) $CNCH_2CO_2Et$, DBU, THF, 25 °C, 12 h, 38%; (e) KOH (powdered), *i*-PrI, DMSO, 25 °C, 1.5 h, 62%; (f) $POCl_3$, DMF, dichloroethane, 80 °C, 3 h, 45%; (g) NaOH, MeOH, 60 °C, 2 h, 100%.

As outlined in Scheme 2, the amide functionality of this class of inhibitors was installed by initial conversion of carboxylic acid **14** to the corresponding acid chloride **15** via treatment with $SOCl_2$. Subsequent reaction of **15** with aniline then afforded anilide **16**. Installation of the 3,5-dihydroxyhexanoic acid side chain was

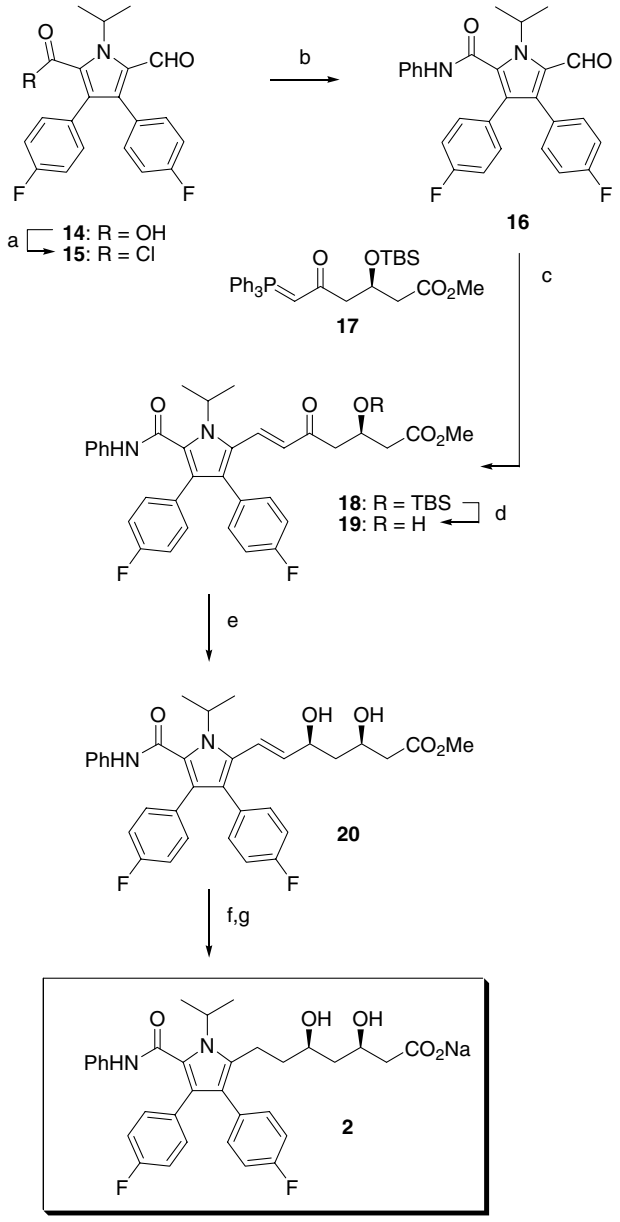

Scheme 2. Synthesis of inhibitor **2**. Reagents and conditions: (a) $SOCl_2$, 80 °C; (b) $PhNH_2$, Et_3N, THF, 25 °C, 12 h, 57% (two steps); (c) toluene, 110 °C, 48 h, 66%; (d) HF (48% in H_2O), MeCN, 0 °C, 2 h, 99%; (e) $Et_2B(OMe)$, $NaBH_4$, AcOH (cat), THF, −78 °C, 2 h, 58%; (f) 10% Pd/C, H_2, EtOH/THF (1:1), 25 °C, 3 h, 100%; (g) NaOH, EtOH, 1 h, 100%.

accomplished via a Wittig olefination reaction between pyrrole carboxaldehyde **16** and stabilized phosphonium yield **17** (prepared stereoselectively in eight steps from diethyl 3-hydroxyglutarate according to the method of Konoike and Araki[16]). In that event, **16** and **17** were reacted at elevated temperature to afford **18** in 66% yield as exclusively the *E*-isomer. The TBS-protected side-chain hydroxyl of **18** was then liberated by treatment with aqueous HF to provide β-hydroxy ketone **19** which was subjected to a stereoselective *syn*-reduction with Et_2-BOMe and $NaBH_4$ to produce syn-diol **20**.[17] Finally, the synthesis was completed by hydrogenation of the side-chain olefin over 10% Pd/C, followed by saponification of the terminal ester to provide compound **2** as its carboxylate sodium salt.

Separately, the route outlined in Schemes 1 and 2 was utilized, with appropriate substitution of alternative building blocks, to prepare all other analogs described in these studies.

Lastly, during the course of this work, a second generation process chemistry synthesis of this class of inhibitors was also developed to facilitate the preparative scale synthesis of selected compounds for pre-clinical efficacy and safety studies. These efforts have been recently reported.[18]

Structural biology. The design of analogs in this series was enabled through structural biology studies beginning with determination of the X-ray structure of inhibitor **2** bound in the active site of HMG-CoA reductase (see Fig. 2).[19] Not surprisingly, inhibitor **2** binds to HMG-CoA in a mode similar to that of other statins [20] with its 3,5-dihydroxyhexanoic acid side chain engaged in an extensive hydrogen bonding network with residues including: Ser-684, Asp-690, Lys-691, Lys 692, Glu 559 and Asp-767. Like both atorvastatin and rosuvastatin, the carbonyl of the amide motif of inhibitor **2** also accepts a hydrogen bond from Ser-556, and the 4-flourophenyl A-Ring of **2** engages in a π-stacking interaction with Arg-590.

Considering the design of novel analogs, examination of Figure 2 revealed that the phenyl ring of the anilide was in a relatively accommodating, and partially solvent-exposed, binding pocket. This suggested that modification at this position might be tolerated and possibly provide an opportunity to modulate inhibitor lipophilicity while still maintaining potency in order to achieve the desired balance between hepatoselectivity and efficacy. This strategy guided our structure–activity optimization studies as described below.

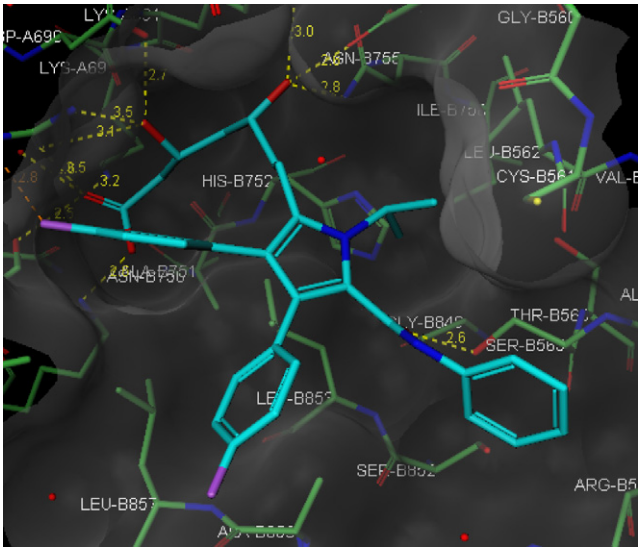

Figure 2. X-ray crystal structure (2.1 Å resolution) of inhibitor **2** bound to the active site of HMG-CoA reductase.

On a separate note, additional inspection of the X-ray structure of Figure 2 revealed, that in its bound conformation, the amide NH-hydrogen and the *ortho*-hydrogen of the phenyl A-ring of inhibitor **2** are in close proximity (1.9 Å) to one another suggesting the possibility of creating an intramolecular connection to create conformationally restricted analogs. This observation is explored in greater detail in the following manuscript.[14b]

Structure–activity studies. Structure–activity studies (Tables 1–4) on this template focused on modification of the amide moiety, since this region was the most synthetically amenable and was anticipated to be tolerant to modification based upon our structural biology studies.

All new analogs were evaluated in an HMG-CoA reductase enzyme inhibition assay.[21] Additionally, the ability of analogs to block cholesterol synthesis in both rat hepatocyte and myocyte cell lines was evaluated, and comparison of these two values was utilized as a measurement of hepatoselectivity. As a guideline, inhibitors with potent hepatocyte activity ($IC_{50} < 10$ nM) and good hepatoselectivity [(myocyte $IC_{50} > 500$ nM) and (myocyte/hepatocyte ratio preferably >1000)] were selected for further evaluation in an acute animal efficacy model. In this model, mice were initially dosed with drug (1 mg/kg) and then, after 0.5 h, given an intraperitoneal injection of ^{14}C sodium acetate. After 4.5 h, a whole blood sample was obtained and analyzed for ^{14}C cholesterol levels which were compared to untreated control animals to determine percent inhibition of acute cholesterol synthesis. Analogs exhibiting acute in vivo activity comparable to or better than the benchmark rosuvastatin (Crestor®) were subsequently evaluated in a chronic LDL-lowering study performed in cholestyramine-primed hamsters. In this study, animals were orally dosed with drug (10 mg/kg) once daily for 7 days. Upon completion of treatment, the percent reduction of serum LDL-C was determined by comparison to an untreated control group. Analogs demonstrating promising single dose efficacy in this model were then evaluated in a full dose–response study to enable an ED_{50} determination.

As shown in Table 1, initial analog efforts focused on the addition of substituents to the anilide ring system as highlighted in Table 1. While the unsubstituted phenyl analogs **2** or **3** had good acute in vivo efficacy, they lacked sufficient selectivity against myocytes with $IC_{50} = 145$ nM and $IC_{50} = 229$ nM, respectively. To improve this selectivity, increasingly hydrophilic substituents were added in an effort to reduce inhibitor lipophilicity. As shown, analogs (**22**–**28**) bearing these polar substituents were less lipophilic ($\mathrm{clog}\,D < 0$) and maintained good activity against HMG-CoA reductase. As expected these more hydrophilic analogs also exhibited good hepatoselectivity with myocyte $IC_{50} > 500$ nM. Unfortunately, achieving this improved selectivity through the addition of polar groups resulted in a concomitant decrease in acute in vivo efficacy as shown. This reduced efficacy was presumably a result of reduced oral absorption due to low membrane permeability. This observation highlighted a key challenge: the balance of selectivity and efficacy.

The evaluation of a series of benzyl amides is highlighted in Table 2. Paralleling the anilide series, the unsubstituted benzyl amide **29** had moderate acute efficacy, but lacked sufficient hepatoselectivity (myocyte $IC_{50} = 44$ nM). The addition of increasingly polar substituents again led to an improvement in selectivity while at the same time generally reducing in vivo efficacy.

Table 1. Structure and biological activity of anilide analogs **2**, **3**, and **21**–**28**[21]

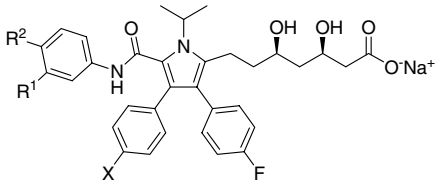

Compound	R^1	R^2	X	HMG-CoA IC_{50} (nM)	Inhibition of cellular cholesterol synthesis		Mouse acute inhibition cholesterol synthesis (1 mg/kg) [%]	$\mathrm{clog}\,D$ (pH 7.4)
					Hepatocyte IC_{50} (nM)	Myocyte IC_{50} (nM)		
Simvastatin				49	1.3	150	−45	4.41
Rosuvastatin				3.1	0.27	250	−82	−2.63
21	OMe	H	F	6.6	0.3	50	−54	0.40
2	H	H	H	12.4	0.4	145	−75	0.31
3	H	H	F	1.8	1.0	229	−57	0.24
22	OH	H	F	0.7	1.2	524	−22	−0.11
23	H	OH	H	0.4	0.5	626	−48	−0.43
24	$C(O)NMe_2$	H	F	0.3	0.2	549	−20	−1.19
25	H	$C(O)NH_2$	H	0.3	0.1	684	−45	−0.73
26	H	$C(O)NMe_2$	H	1.4	0.7	1110	−10	−1.04
27	H	SO_2NH_2	H	2.9	0.3	1790	−32	−0.88
28	H	CO_2H	H	0.3	0.1	12,600	NA	−1.29

NA, not active.

Table 2. Structure and biological activity of benzyl amide analogs **29**–**36**[21]

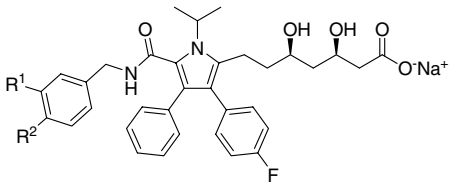

Compound	R^1	R^2	HMG-CoA IC_{50} (nM)	Inhibition of cellular cholesterol synthesis		Mouse acute inhibition cholesterol synthesis (1 mg/kg) [%]	clog*D* (pH 7.4)
				Hepatocyte IC_{50} (nM)	Myocyte IC_{50} (nM)		
Simvastatin			49	1.3	150	−45	4.41
Rosuvastatin			3.1	0.27	250	−82	−2.63
29	H	H	0.8	0.3	44	−46	1.77
30	H	OMe	0.8	0.4	310	−52	1.68
31	H	CH_2OMe	0.7	1.5	211	—	1.51
32	OMe	H	1.8	0.1	130	—	1.68
33	H	CN	0.2	0.7	650	−47	1.21
34	$C(O)NH_2$	H	1.2	0.1	3100	−22	0.29
35	H	$C(O)NMe_2$	1.2	4.9	6520	−38	0.01
36	H	CO_2H	2.2	0.1	7920	−7	−0.27

Table 3. Structure and biological activity of heterocyclic amide analogs **37**–**41**[21]

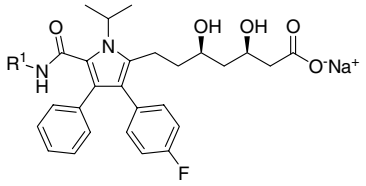

Compound	R^1	HMG-CoA IC_{50} (nM)	Inhibition of cellular cholesterol synthesis		Mouse acute inhibition cholesterol synthesis (1 mg/kg) [%]	clog*D* (pH 7.4)
			Hepatocyte IC_{50} (nM)	Myocyte IC_{50} (nM)		
Simvastatin		49	1.3	150	−45	4.41
Rosuvastatin		3.1	0.3	250	−82	−2.63
29	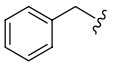	0.8	0.3	44	−46	1.77
37	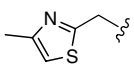	1.5	1.5	1010	−33	1.16
38	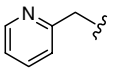	0.8	0.1	472	−39	0.28
39	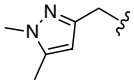	0.6	0.9	3230	−19	0.18
40	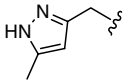	2.6	0.5	10,400	N/A	0.33
41	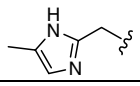	3.4	0.5	10,400	−11	−0.03

Table 4. Structure and biological activity of alkyl amide analogs **42**–**47**[21]

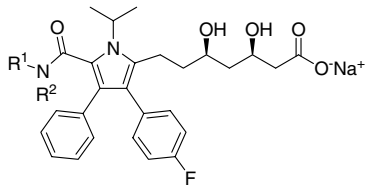

Compound	R^1	R^2	HMG-CoA IC_{50} (nM)	Inhibition of cellular cholesterol synthesis		Mouse acute inhibition cholesterol synthesis (1 mg/kg) [%]	Hamster 7-day LDL-lowering (10 mg/kg) [%]	clog *D* (pH 7.4)
				Hepatocyte IC_{50} (nM)	Myocyte IC_{50} (nM)			
Simvastatin			49	1.3	150	−45	—	4.41
Rosuvastatin			3.1	0.27	250	−82	−25	−2.63
42	H	H	3.0	0.6	2450	−85	−11	−0.48
43	H	Me	8.8	1.2	5300	−83	−12	−0.32
44	H	Et	12	0.7	2270	−76	−24	−0.21
45	Me	Me	20	0.9	1580	−85	—	−1.87
46	H	*i*-Pr	15	1.6	1930	−73	—	0.56
47	H	*c*-Pr	3.8	2.0	2780	−70	−24	0.05

In an effort to influence the selectivity/efficacy balance without the use of polar substituents, we next evaluated a series of heterocyclic amides as outlined in Table 3. Encouragingly, nearly all of these analogs (**37**–**41**) exhibited good hepatoselectivity; unfortunately, all compounds had inferior acute efficacy relative to the benchmark compounds.

As shown in Table 4, we also evaluated whether or not non-aromatic amides would afford the desired balance of selectivity and efficacy. Interestingly, primary (**42**), secondary alkyl (**43**, **44**, **46**, **47**) and tertiary alkyl amides (**45**) all demonstrated excellent hepatoselectivity with myocyte $IC_{50} > 1000$ nM. Furthermore, all of the analogs in this series exhibited significant acute efficacy relative to the benchmark standards.

In order to further characterize the therapeutic potential of the primary and alkyl amides of Table 4 (**42**–**47**) we evaluated these analogs in a 7-day LDL-lowering assay conducted in cholestyramine-primed hamsters. Initially, analogs were evaluated at a single oral dose of 10 mg/kg and compared against the benchmark rosuvastatin at the same dose. As highlighted in Table 4, compounds **44** and **47** exhibited comparable efficacy to rosuvastatin at this dose. Metabolic stability studies (data not shown) suggested that **44** was more metabolically robust than **47**, and as such **44** was selected for a full dose–response study in this hamster model. Doses of 0.1, 0.5, 1, 5, 10, and 50 mg/kg of **44** were evaluated in separate animal groups ($n = 10$ each) resulting in an $ED_{50} = 3$ mg/kg for this inhibitor. For comparison purposes, rosuvastatin was evaluated at a dose of 10 mg/kg in an additional animal group during this study. As illustrated, **44** and rosuvastatin exhibited similar efficacies at this dose (Fig. 3).

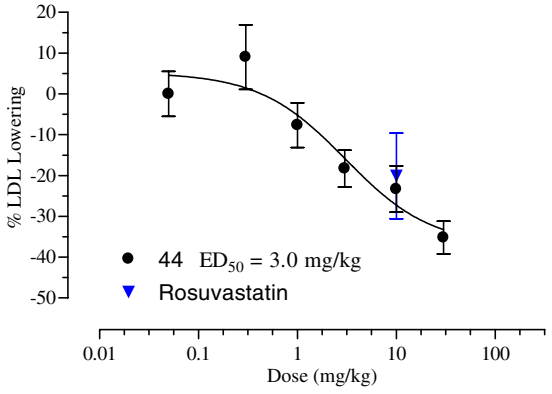

Figure 3. Effect of **44** on plasma LDL in hamsters dosed orally for 7 days. All groups were sacrificed 2 h post-dose on the final day of dosing. Data represent means ± SEM of the percent change from the control group ($n = 10$/group). Rosuvastatin was tested in a similar manner at a dose of 10 mg/kg.

In conclusion, we have described the design, synthesis, and biological evaluation of a series of pyrrole-based HMG-CoA reductase inhibitors based upon an isomeric variation of the atorvastatin template. Through structure–activity studies, we identified a subset of alkyl amide containing analogs that exhibited excellent hepatoselectivity as well as good acute and chronic efficacy in animal models of dyslipidemia. Of particular interest was inhibitor **44** which was 3200-fold selective for inhibiting cholesterol synthesis in hepatocytes as opposed to myocytes, yet it maintained pre-clinical LDL-lowering efficacy comparable to that of rosuvastatin. It is anticipated that additional pre-clinical characterization of this compound will represent an important step in the identification of a next generation HMG-CoA reductase inhibitor useful for helping patients to achieve increasingly aggressive LDL-lowering goals.

Acknowledgments

We acknowledge the technical contributions made by Fang Sun, Loola Al-Kassim, Susan Holly, Cindy

Spessard, and Siradanahalli Guru. We also thank Barry Finzel for his assistance with the X-ray structure.

References and notes

1. American Heart Association Statistics Committee and Stroke Statistics Subcommittee, 2007 Update. Dallas, TX: American Heart Association, 2007.
2. (a) LaRosa, J. C.; Grundy, S. M.; Walters, D. D.; Shear, C.; Barter, P.; Fruchart, J.-C.; Gotto, A. M.; Greten, H.; Kastelein, J. J. P.; Shepard, J.; Wenger, N. K. *N. Engl. J. Med.* **2005**, *352*, 1425; (b) Schwartz, G.; Olsson, A. G.; Ezekowitz, M. D.; Ganz, P.; Oliver, M. F.; Waters, D.; Zeiher, A.; Chaitman, B. R.; Leslie, S.; Stern, T. *JAMA* **2001**, *285*, 1711; (c) Cannon, C. P.; Braunwald, E.; McCabe, C. H.; Rader, D. J.; Rouleau, J. L.; Belder, R.; Joyal, S. V.; Hill, K.; Pfeffer, M. A.; Skene, A. M. *N. Engl. J. Med.* **2004**, *350*, 1495.
3. For a review, see: (a) McKenney, J. M. *Clin. Cardiol.* **2003**, *26*(Suppl. III), 32.
4. (a) Scandinavian Simvastatin Survival Study Investigators. Lancet, 1994, 344, 1383; (b) The long-term intervention with pravastatin in ischemic disease (LIPID) study group. *N. Engl. J. Med.* **1998**, *339*, 1349; (c) Shepard, J.; Cobbe, S. M.; Ford, I.; Isles, C. G.; Lorimer, A. R.; MacFarlane, P. W.; McKillop, J. H.; Pachard, C. J. *N. Engl. J. Med.* **1995**, *333*, 1301; (d) LaRosa, J. C.; He, J.; Vupputuri, S. *JAMA* **1999**, *282*, 2340.
5. (a) LaRosa, J. C.; Grundy, S. M.; Walters, D. D.; Shear, C.; Barter, P.; Fruchart, J.-C.; Gotto, A. M.; Greten, H.; Kastelein, J. J. P.; Shepard, J.; Wenger, N. K. *N. Engl. J. Med.* **2005**, *352*, 1425; (b) Schwartz, G.; Olsson, A. G.; Ezekowitz, M. D.; Ganz, P.; Oliver, M. F.; Waters, D.; Zeiher, A.; Chaitman, B. R.; Leslie, S.; Stern, T. *JAMA* **2001**, *285*, 1711; (c) Cannon, C. P.; Braunwald, E.; McCabe, C. H.; Rader, D. J.; Rouleau, J. L.; Belder, R.; Joyal, S. V.; Hill, K.; Pfeffer, M. A.; Skene, A. M. *N. Engl. J. Med.* **2004**, *350*, 1495.
6. Grundy, S. M.; Cleeman, J. I.; Merz, N. B.; Brewer, B.; Clark, L. T.; Hunninghake, D. B.; Pasternak, R. C.; Smith, S. C.; Stone, N. J. *Circulation* **2004**, *110*, 227.
7. O'Keefe, J. H.; Cordain, L.; Harris, W. H.; Moe, R. M.; Vogel, R. *J. Am. Coll. Cardiol.* **2004**, *43*, 2142.
8. For a review, see Patel, T. N.; Shishehbor, M. H.; Bhatt, D. L. *Eur. Heart J.* **2007**, *28*, 664.
9. (a) Brukert, E.; Hayem, G.; Dejager, S.; Yau, C.; Begaud, B. *Cardiovasc. Drugs Ther.* **2005**, *19*, 403; (b) Baer, A. N.; Wortmann, R. L. *Curr. Opin. Rheumatol.* **2007**, *19*, 67; (c) Tiwari, A.; Bansal, V.; Chugh, A.; Mookhtiar, K. *Expert Opin. Drug Saf.* **2006**, *5*, 651; (d) Athar, H.; Shah, A. R.; Thompson, P. D. *Future Lipidol.* **2006**, *1*, 143; (e) Franc, S.; Dejager, S.; Bruckert, E.; Chauvenet, M.; Giral, P.; Turpin, G. *Cardiovasc. Drugs Ther.* **2003**, *17*, 459.
10. (a) Hamelin, B. A.; Turgeon, J. *Trends Pharm Sci.* **1998**, *19*, 26; (b) Rosenson, R. S.; Tangney, C. C. *JAMA* **1998**, *279*, 1643; See also (c) Schachter, M. *Fundam. Clin. Pharmacol.* **2004**, *19*, 117; (d) Ho, R. H.; Tirona, R. G.; Leake, B. F.; Glaeser, H.; Lee, W.; Lemke, C. J.; Wang, Y.; Kim, R. B. *Gastroenterology* **2006**, *130*, 1793.
11. (a) Roth, B. D.; Bocan, T. M.; Blankey, C. J.; Chucholowski, A. W.; Creger, P. L.; Creswell, M. W.; Ferguson, E.; Newton, R. S.; O'Brien, P.; Picard, J. A.; Roark, W. H.; Sekerke, C. S.; Sliskovic, D. R.; Wilson, M. W. *J. Med. Chem.* **1991**, *34*, 466; (b) Koga, T.; Shimada, Y.; Kuroda, M.; Tsujita, Y.; Hasegawa, K.; Yamazaki, M. *Biochim. Biophys. Acta* **1990**, *1045*, 115; (c) Balasubramanian, N.; Brown, P. J.; Catt, J. D.; Han, W. T.; Parker, R. A.; Sit, S. Y.; Wright, J. J. *J. Med. Chem.* **1989**, *32*, 2038; (d) Joshi, H. N.; Fakes, M. G.; Serajuddin, A. M. *Pharm. Pharmacol. Commun.* **1999**, *5*, 267.
12. Hsiang, B.; Zhu, Y.; Wang, Z.; Wu, Y.; Sasseville, V.; Yang, W.-P.; Kirchgessner, T. G. *J. Biol. Chem.* **1999**, *274*, 37161.
13. The use of other heterocyclic cores will be described in separate, forthcoming reports.
14. (a) For additional studies on this pyrrole template, see: Bratton, L. D.; Auerbach, B.; Choi, C.; Dillon, L.; Hanselman, J. C.; Larsen, S. D.; Lu, G.; Olsen, K.; Pfefferkorn, J. A.; Robertson, A.; Sekerke, C.; Trivedi, B. K.; Unangst, P. C. *Bioorg. Med. Chem.* **2007**, in press. doi:10.1016/j.bmc.2007.05.031; (b) Pfefferkorn, J. A.; Choi, C.; Song, Y.; Trivedi, B. K.; Larsen, S. D.; Askew, V.; Dillon, L.; Hanselman, J. C.; Lin, Z.; Lu, G.; Robertson, A.; Sekerke, C.; Auerbach, B.; Pavlovsky, A.; Harris, M. S.; Bainbridge, G.; Caspers, N. *Bioorg. Med. Chem. Lett.* **2007**, in press. doi:10.1016/j.bmcl.2007.05.097.
15. Barton, D. H. R.; Zard, S. C. *Chem. Commun.* **1985**, 1098.
16. Konoike, T.; Araki, Y. *J. Org. Chem.* **1994**, *59*, 7849.
17. Chen, K.-M.; Hardtmann, G. E.; Prasad, K.; Repic, O.; Shapiro, M. J. *Tetrahedron Lett.* **1987**, *28*, 155.
18. Pfefferkorn, J. A.; Bowles, D. M.; Kissel, W.; Bolyles, D. C.; Choi, C.; Larsen, S. D.; Song, Y.; Sun, K.-L.; Miller, S.; Trivedi, B. K. *Tetrahedron*, in press.
19. The structure of HMG-CoA reductase (HMGR) in complex with statins has previously been reported (see Ref. 20). For the purpose of this study a modified version of the published clone was used. Briefly HMGR was expressed as an N-terminal His 6 protein truncated from amino acid 441–875 with the mutation M485I in the *E. coli* strain BL21 STAR. Protein was purified via Ni-affinity and gel filtration chromatography. HMGR was concentrated to 20 mg/ml then complexed with statins at a concentration of 0.5mM and incubated at 4 °C for 1 h. Crystals were prepared in hanging drops from a crystallization solution of 28% PEG 4000, 0.1 mM Tris, pH 8.5, 0.2 M LiSO4, and 50 mM DTT at 20 °C. Diffraction quality crystals (P21) were obtained after micro-seeding, harvested after 1 week, and cryo protected in 25% ethylene glycol. Data were collected at 2 Å resolution at the Industrial Macromolecular Crystallography Association Collaborative Access Team (IMCA-CAT) beam-line ID-17 at the Advanced Photon Source (Argonne National Laboratory). All data were processed and scaled using HKL2000. Data for Figure 2 have been deposited at the PDB under filename 2Q1L.
20. (a) Istvan, E. S.; Deisenhofer, J. *Science* **2001**, *292*, 1160; (b) Istvan, E. *Atherosclerosis Suppl.* **2003**, *4*, 3.
21. In vitro IC_{50} values are reported as arithmetic means for $n \geqslant 2$ independent measurements unless otherwise noted. In vivo measurements are represented as the percent change from untreated control group ($n = 10$ animals/group). For detailed assay protocols, see Ref. 14a.